Postprint of: Morawiec M., Z type Observer Backstepping For Induction Machines, IEEE TRANSACTIONS ON INDUSTRIAL ELECTRONICS, Vol. 62, Iss. 4 (2015), pp. 2090-2102, DOI: 10.1109/TIE.2014.2355417



# Z–Type Observer Backstepping For Induction Machines

Marcin Morawiec

***Abstract*—This paper contains a relatively new synthesis method for non-linear objects, named backstepping. This method can be used to obtain the observer structure. The paper presents the structure of the speed observer which is a new proposition of observer backstepping with additional state variables marked *Z*. The rotor speed can be estimated in three different ways. The first is based on the adaptive approach, the second on the non-adaptive approach, and the third on improvement of the adaptive approach. The stability of the Z-type observer is determined by the Lyapunov stability criteria. Despite this, stability analysis around the machine's working point is undertaken. All the machine tests are prepared in the sensorless control system based on multi-scalar variables. The experimental results show the effectiveness of the proposed solution. The squirrel-cage model parameter estimation is not presented in this paper.**

***Index Terms*— Adaptive observers, AC machines, Backstepping.**

## Nomenclature

| | |
|---|---|
| "^" | estimated values, |
| "~" | error of estimated values, |
| $i_{s\alpha,\beta}$ | stator current vector components, |
| $\psi_{r\alpha,\beta}$ | rotor flux vector components, |
| $u_{s\alpha,\beta}$ | stator voltage vector components, |
| $\omega_r$ | rotor angular speed, |
| $R_r$, $R_s$ | rotor and stator resistances, |
| $L_m$ | mutual-flux inductance, |
| $L_s$, $L_r$ | stator and rotor inductances, |
| $T_L$ | load torque, |
| $J$ | machine torque of inertia, |
| $\tau$ | relative time, |
| $\hat{\omega}_r$ | estimated rotor electrical speed, |
| $\tilde{\omega}_r$ | rotor speed error, |
| $\tilde{\psi}_{r\alpha,\beta}$ | rotor flux vector components error, |
| $\tilde{i}_{s\alpha,\beta}$ | stator current vector components error, |
| $\hat{Z}_{\alpha,\beta}$ | additional observer state variables, |
| $v_{\alpha,\beta}$ | speed observer stabilizing variables, |
| $c_{\alpha,\beta}$ | constant coefficients, |
| $x_{11}$, $x_{12}$, $x_{21}$, $x_{22}$ | multi-scalar variables. |

Manuscript received March 5, 2014; revised March 10, 2014, May 26, 2014 and July 20, 2014; accepted July 29, 2014.



## I. Introduction

Modern drive systems possess both a speed sensor and a speed observer. Control systems with a speed observer are called "sensorless". The speed observer of the squirrel-cage machine is supposed to reconstruct the following state variables: the rotor flux vector and the stator current vector components. Sometimes, the rotor speed in the estimator can be treated as an additional parameter. Good performance estimators should reconstruct these state variables with steady state errors smaller than 1% and dynamic state errors smaller than 5%. The most popular observer is that based on Luenberger's theory [1–3]. Recently, the Luenberger observer was extended to another form. In [2–3], the Luenberger observer was extended to additional variables, which are, in this case, the state variables. The additional state variables are the product of the rotor angular speed and the proper flux vector components.

The following large group of estimators is based on the Kalman filter [4–6]. The main disadvantage of using the Kalman filter is the large computational cost. To reduce the computing time, the gain matrix is computed off-line.

The next group are observers based on fuzzy logic or neural network theory with the backstepping approach. These ideas of estimators are presented in [7–17]. Some of them have a hybrid structure, meaning there is a connection between the adaptive and neural network estimations.

The fourth group of estimators are the adaptive observers using MRAS (model reference adaptive system) methods or the backstepping approach. The most popular MRAS idea is based on a current and voltage mathematical model of a machine [18].

This paper concerns the estimators of state variables and the rotor angular speed of an induction machine design for the adaptive backstepping concept [7–17, 19–35–38]. The primary estimator model extension leads to additional differentiation equations. When the adaptive backstepping method is applied, stabilizing elements can be obtained by the proper use of the Lyapunov function [19]. In [19], adaptive backstepping observer stability is proved and the stability range is given. The properties of the proposed Z-type observer will be compared to the adaptive observer backstepping. The primary advantages of the use of the Z-type observer will be shown in the following sections.

The paper focuses on emphasizing the advantages of the proposed Z-type adaptive observer backstepping structure and comparing it to the standard adaptive observer backstepping.

The main motivation of the paper is to show the new structure of observer backstepping which can work under very low machine speeds (stable). This paper may lead to a new approach to estimators, namely the control theory approach based on the separation of the new variables in the control object, which will be treated as state variables describing the object state. The extended object model gives new possibilities for parameter or state variable estimation.

All the discussions of theoretical issues are supported by simulation and experimental studies.

## II. The Basis of Integrator Backstepping

According to the definition presented in [19] for the system $\dot{x} = f(x) + g(x)u$ feedback control law exists such that $u = \alpha(x)$ and positive radially unbounded function *V(x)*. According to [19-Lemma 2.8] the system $\dot{x} = f(x) + g(x)u$ can be augmented by the integrator structure such that:

$$\dot{x} = f(x) + g(x)\xi, \tag{1}$$

$$\dot{\xi} = u, \tag{2}$$

where $\xi$ is the control in the system and $u$ can be chosen as the virtual control.

The first step in the backstepping procedure is to define the new tracking error between the virtual control $u = \alpha(x)$ and the desired $\xi$. The tracking error is defined as:

$$z = \xi - \alpha(x). \tag{3}$$

Calculation of the deviation derivatives of (3) gives:

$$\dot{z} = \dot{\xi} - \dot{\alpha}(x). \tag{4}$$

Using (4) the system (1)–(2) can be transformed to the *(x,ξ,z)* coordinates. The system in *(x,ξ,z)* will be stable if the Lyapunov condition is satisfied:

$$\dot{V}(\xi, x, z) \le 0. \tag{5}$$

From (5) the control variable *u* can be obtained. The control *u* guarantees the asymptotical stability of the system (1)–(2).

The same procedure can be implemented with the speed observer. Assuming the only one measured value is the stator current vector components and the machine control variables ($u_{s\alpha,\beta}$) are known, the integrators take the form:

$$\dot{\xi}_{\alpha,\beta} = \tilde{i}_{s\alpha,\beta}, \tag{6}$$

$$\tilde{i}_{s\alpha,\beta} = \hat{i}_{s\alpha,\beta} - i_{s\alpha,\beta}, \tag{7}$$

where $\hat{i}_{s\alpha,\beta}$ are the estimated stator current vector components.

In the next section the primary observer structure will be augmented by the integrators (6). The next step in the backstepping procedure is to determine which of the feedback coupling controls *v* (correction terms) can stabilize the observer structure such that the Lyapunov condition will be fulfilled (5).

## III. The Mathematical Model of the Induction Motor

The equations of the induction squirrel-cage machine, written in a stationary (*αβ*) reference frame, have the following form [2–3]:

$$\frac{di_{s\alpha}}{d\tau} = -\frac{R_s L_r^2 + R_r L_m^2}{L_r w_\sigma} i_{s\alpha} + \frac{R_r L_m}{L_r w_\sigma} \psi_{r\alpha} + \omega_r \frac{L_m}{w_\sigma} \psi_{r\beta} + \frac{L_r}{w_\sigma} u_{s\alpha}, \tag{8}$$

$$\frac{di_{s\beta}}{d\tau} = -\frac{R_s L_r^2 + R_r L_m^2}{L_r w_\sigma} i_{s\beta} + \frac{R_r L_m}{L_r w_\sigma} \psi_{r\beta} - \omega_r \frac{L_m}{w_\sigma} \psi_{r\alpha} + \frac{L_r}{w_\sigma} u_{s\beta}, \tag{9}$$

$$\frac{d\psi_{r\alpha}}{d\tau} = -\frac{R_r}{L_r} \psi_{r\alpha} - \omega_r \psi_{r\beta} + \frac{R_r L_m}{L_r} i_{s\alpha}, \tag{10}$$

$$\frac{d\psi_{r\beta}}{d\tau} = -\frac{R_r}{L_r} \psi_{r\beta} + \omega_r \psi_{r\alpha} + \frac{R_r L_m}{L_r} i_{s\beta}, \tag{11}$$

$$\frac{d\omega_r}{d\tau} = \frac{L_m}{JL_r} (\psi_{r\alpha} i_{s\beta} - \psi_{r\beta} i_{s\alpha}) - \frac{1}{J} T_L, \tag{12}$$

where:

$$w_\sigma = L_r L_s - L_m^2.$$

## IV. Z–type Speed Observer Backstepping

### A. State variables estimation using backstepping

The mathematical model (8)–(12) contains five differential equations. In the backstepping procedure, Equation (12) can be omitted because the rotor angular speed is treated as an estimated parameter.

Proceeding in accordance with the adaptive estimator with the integrator backstepping concept (presented in Section II), one can derive formulae for the observer, where only the state variables will be estimated, as well as the rotor angular speed as an additional estimation parameter.

The estimated values will be indexed by "^" and their deviations (prediction errors [21, 28]) by "~".

Treating the stator current vector components $i_{s\alpha,\beta}$ in (8)–(9) as the measured values and stator voltage components $u_{s\alpha,\beta}$ as the known values, the standard exponential observer structure is obtained:

$$\frac{d\hat{i}_{s\alpha}}{d\tau} = -\frac{R_s L_r^2 + R_r L_m^2}{L_r w_\sigma} i_{s\alpha} + \frac{R_r L_m}{L_r w_\sigma} \hat{\psi}_{r\alpha} + \hat{\omega}_r \frac{L_m}{w_\sigma} \hat{\psi}_{r\beta} + \frac{L_r}{w_\sigma} u_{s\alpha} + v_\alpha, \tag{13}$$

$$\frac{d\hat{i}_{s\beta}}{d\tau} = -\frac{R_s L_r^2 + R_r L_m^2}{L_r w_\sigma} i_{s\beta} + \frac{R_r L_m}{L_r w_\sigma} \hat{\psi}_{r\beta} - \hat{\omega}_r \frac{L_m}{w_\sigma} \hat{\psi}_{r\alpha} + \frac{L_r}{w_\sigma} u_{s\beta} + v_\beta, \tag{14}$$

$$\frac{d\hat{\psi}_{r\alpha}}{d\tau} = -\frac{R_r}{L_r} \hat{\psi}_{r\alpha} - \hat{\omega}_r \hat{\psi}_{r\beta} + \frac{R_r L_m}{L_r} i_{s\alpha} + v_{\psi\alpha}, \tag{15}$$

$$\frac{d\hat{\psi}_{r\beta}}{d\tau} = -\frac{R_r}{L_r} \hat{\psi}_{r\beta} + \hat{\omega}_r \hat{\psi}_{r\alpha} + \frac{R_r L_m}{L_r} i_{s\beta} + v_{\psi\beta}. \tag{16}$$

where: $\hat{\omega}_r$ is the estimated angular rotor speed and the remaining errors are defined by:

$$\tilde{\omega}_r = \hat{\omega}_r - \omega_r, \tag{17}$$

$$\tilde{\psi}_{r\alpha,\beta} = \hat{\psi}_{r\alpha,\beta} - \psi_{r\alpha,\beta}. \tag{18}$$

In (13)–(14), the correction terms $v_{\alpha,\beta}$ and $v_{\psi\alpha,\beta}$ are added to the current and the flux subsystem.

The standard exponential observer structure can be extended to additional variables that will be treated as the state variables. Such an approach was proposed in [2, 3].

In this paper the same variables as in [2, 3] are named *Z* and determined as follows:

$$\hat{Z}_\alpha = \hat{\omega}_r \hat{\psi}_{r\alpha}, \tag{19}$$

$$\hat{Z}_\beta = \hat{\omega}_r \hat{\psi}_{r\beta}. \tag{20}$$

Taking into account (19)–(20) in the structure (13)–(16), differentiating (19)–(20), the new Z-type structure is obtained:

$$\frac{d\hat{i}_{s\alpha}}{d\tau}=-\frac{R_sL_r^2+R_rL_m^2}{L_rw_\sigma}i_{s\alpha}+\frac{R_rL_m}{L_rw_\sigma}\hat{\psi}_{r\alpha}+\frac{L_m}{w_\sigma}\hat{Z}_\beta+\frac{L_r}{w_\sigma}u_{s\alpha}+v_\alpha, \quad (21)$$

$$\frac{d\hat{i}_{s\beta}}{d\tau}=-\frac{R_sL_r^2+R_rL_m^2}{L_rw_\sigma}i_{s\beta}+\frac{R_rL_m}{L_rw_\sigma}\hat{\psi}_{r\beta}-\frac{L_m}{w_\sigma}\hat{Z}_\alpha+\frac{L_r}{w_\sigma}u_{s\beta}+v_\beta, \quad (22)$$

$$\frac{d\hat{\psi}_{r\alpha}}{d\tau}=-\frac{R_r}{L_r}\hat{\psi}_{r\alpha}-\hat{Z}_\beta+\frac{R_rL_m}{L_r}i_{s\alpha}+v_{\psi\alpha}, \quad (23)$$

$$\frac{d\hat{\psi}_{r\beta}}{d\tau}=-\frac{R_r}{L_r}\hat{\psi}_{r\beta}+\hat{Z}_\alpha+\frac{R_rL_m}{L_r}i_{s\beta}+v_{\psi\beta}, \quad (24)$$

$$\frac{d\hat{Z}_\alpha}{d\tau}=\frac{d\hat{\omega}_r}{d\tau}\hat{\psi}_{r\alpha}-\hat{\omega}_r(\hat{Z}_\beta-\frac{R_rL_m}{L_r}i_{s\alpha})+\frac{R_r}{L_r}\hat{Z}_\alpha+v_{Z\alpha}, \quad (25)$$

$$\frac{d\hat{Z}_\beta}{d\tau}=\frac{d\hat{\omega}_r}{d\tau}\hat{\psi}_{r\beta}+\hat{\omega}_r(\hat{Z}_\alpha+\frac{R_rL_m}{L_r}i_{s\beta})+\frac{R_r}{L_r}\hat{Z}_\beta+v_{Z\beta}, \quad (26)$$

where the new correction terms $v_{Z\alpha,\beta}$ are added to the Z-subsystem. In (25)–(26) it can be assumed that: $\frac{d\hat{\omega}_r}{d\tau}\approx\frac{\Delta\hat{\omega}_r}{\Delta T}\approx 0$. The Z-type observer structure contains the three subsystems: the stator current subsystem giving (21)–(22), the rotor flux vector giving (23)–(24) and the Z-type determined by (25)–(26). The current subsystem values are stabilized by $v_{\alpha,\beta}$. The flux vector subsystem controls are stabilized by $v_{\psi\alpha,\beta}$. In the Z-subsystem the stabilizing functions are $v_{Z\alpha,\beta}$.

The observer correction terms will be determined by the backstepping procedure in such a way as to satisfy the Lyapunov condition (5). The variables (19)–(20) are the new induction machine state variables which will be used to reconstruct the induction machine angular speed.

Assuming the strict output-feedback form in which the stator current vector components are only measured using (21)–(26) and the extended machine model (the dependences (21)–(26) without "^" and the correction terms), the deviations model has the form:

$$\frac{d\tilde{i}_{s\alpha}}{d\tau}=\frac{R_rL_m}{L_rw_\sigma}\tilde{\psi}_{r\alpha}+\frac{L_m}{w_\sigma}\tilde{Z}_\beta+v_\alpha, \quad (27)$$

$$\frac{d\tilde{i}_{s\beta}}{d\tau}=\frac{R_rL_m}{L_rw_\sigma}\tilde{\psi}_{r\beta}-\frac{L_m}{w_\sigma}\tilde{Z}_\alpha+v_\beta, \quad (28)$$

$$\frac{d\tilde{\psi}_{r\alpha}}{d\tau}=-\frac{R_r}{L_r}\tilde{\psi}_{r\alpha}-\tilde{Z}_\beta+v_{\psi\alpha}, \quad (29)$$

$$\frac{d\tilde{\psi}_{r\beta}}{d\tau}=-\frac{R_r}{L_r}\tilde{\psi}_{r\beta}+\tilde{Z}_\alpha+v_{\psi\beta}, \quad (30)$$

$$\frac{d\tilde{Z}_\alpha}{d\tau}=-\hat{\omega}_r\tilde{Z}_\beta-\tilde{\omega}_r\hat{Z}_\beta+\tilde{\omega}_r\tilde{Z}_\beta+\tilde{\omega}_r\frac{R_rL_m}{L_r}i_{s\alpha}+\frac{R_r}{L_r}\tilde{Z}_\alpha+v_{Z\alpha}, \quad (31)$$

$$\frac{d\tilde{Z}_\beta}{d\tau}=\hat{\omega}_r\tilde{Z}_\alpha+\tilde{\omega}_r\hat{Z}_\alpha-\tilde{\omega}_r\tilde{Z}_\alpha+\tilde{\omega}_r\frac{R_rL_m}{L_r}i_{s\beta}+\frac{R_r}{L_r}\tilde{Z}_\beta+v_{Z\beta}. \quad (32)$$

In accordance with the integrator backstepping approach (presented in Section II), the additional integrators of the current stator vector errors are used. The stator current errors are chosen rather than integrators because the stator current components are measured. The observer backstepping with the integrators has a simpler form than the one with the filters (presented in [19]) and a smaller observer order.

For the stator current vector components the integrators are defined as follows (6):

$$\frac{d\tilde{\xi}_\alpha}{d\tau}=\tilde{i}_{s\alpha}, \quad (33)$$

$$\frac{d\tilde{\xi}_\beta}{d\tau}=\tilde{i}_{s\beta}, \quad (34)$$

The first step in the backstepping procedure is to stabilize the integrators (and the system by the integrators). The stabilizing function should be chosen so as to satisfy the Lyapunov condition. The Lyapunov function is determined:

$$V_1(\tilde{\xi}_{\alpha,\beta})=\frac{1}{2}(\tilde{\xi}_\alpha^2+\tilde{\xi}_\beta^2). \quad (35)$$

The derivative of (35) takes the form:

$$\dot{V}_1(\tilde{\xi}_{\alpha,\beta})=-c_\alpha\tilde{\xi}_\alpha^2-c_\alpha\tilde{\xi}_\beta^2+\tilde{\xi}_\alpha(\tilde{i}_{s\alpha}+c_\alpha\tilde{\xi}_\alpha)+\tilde{\xi}_\beta^2(\tilde{i}_{s\beta}+c_\alpha\tilde{\xi}_\beta)\le 0. \quad (36)$$

The condition will be fulfilled if the stabilizing function $\sigma_{\alpha,\beta}$:

$$\sigma_\alpha=\tilde{i}_{s\alpha}=-c_\alpha\tilde{\xi}_\alpha, \quad (37)$$

$$\sigma_\beta=\tilde{i}_{s\beta}=-c_\alpha\tilde{\xi}_\beta. \quad (38)$$

The second step in the backstepping procedure is introducing the deviation variables "z". The desired values are the stabilizing functions $\sigma_\alpha$, $\sigma_\beta$ and the virtual control is $\tilde{i}_{s\alpha,\beta}$. The deviations are defined:

$$z_\alpha=\tilde{i}_{s\alpha}+c_\alpha\tilde{\xi}_\alpha, \quad (39)$$

$$z_\beta=\tilde{i}_{s\beta}+c_\alpha\tilde{\xi}_\beta. \quad (40)$$

Using (39)–(40) the integrator dependences (33)–(34) take the form:

$$\frac{d\tilde{\xi}_\alpha}{d\tau}=z_\alpha-c_\alpha\tilde{\xi}_\alpha, \quad (41)$$

$$\frac{d\tilde{\xi}_\beta}{d\tau}=z_\beta-c_\alpha\tilde{\xi}_\beta. \quad (42)$$

Defining the deviations "z" and taking into account (41)–(42) the back-step through the integrator was achieved [19].

Calculation of the (39)–(40) deviation derivatives gives:

$$\dot{z}_\alpha=\frac{R_rL_m}{L_rw_\sigma}\tilde{\psi}_{r\alpha}+\frac{L_m}{w_\sigma}\tilde{Z}_\beta+v_\alpha+c_\alpha\tilde{i}_{s\alpha}, \quad (43)$$

$$\dot{z}_\beta=\frac{R_rL_m}{L_rw_\sigma}\tilde{\psi}_{r\beta}-\frac{L_m}{w_\sigma}\tilde{Z}_\alpha+v_\beta+c_\alpha\tilde{i}_{s\beta}. \quad (44)$$

By selecting the following Lyapunov function:

$$V(\tilde{\xi}_\alpha,\tilde{\xi}_\beta,z_\alpha,z_\beta,\tilde{\psi}_\alpha,\tilde{\psi}_\beta,\tilde{Z}_\alpha,\tilde{Z}_\beta)=\frac{1}{2}(\tilde{\xi}_\alpha^2+\tilde{\xi}_\beta^2+z_\alpha^2+z_\beta^2+ +\tilde{\psi}_\alpha^2+\tilde{\psi}_\beta^2+\tilde{Z}_\alpha^2+\tilde{Z}_\beta^2), \quad (45)$$

calculating the derivative and substituting the respective expressions, new correction terms can be determined. The Lyapunov function is determined for the dynamics of the $\xi_{\alpha,\beta}$, $z_{\alpha,\beta}$ variables and for the rotor flux components. Calculating the derivatives (45) and substituting (29)–(32) and (43)–(44), one obtains:

$$\begin{aligned}\dot{V} &= -c_\beta z_\alpha^2 - c_\beta z_\beta^2 - \frac{R_r}{L_r}(\tilde{\psi}_{r\alpha}^2 + \tilde{\psi}_{r\beta}^2) + z_\alpha(\frac{R_r L_m}{L_r w_\sigma}\tilde{\psi}_{r\alpha} + \frac{L_m}{w_\sigma}\tilde{Z}_\beta + \\ &+ v_\alpha + c_\beta z_\alpha + c_\alpha \tilde{i}_{s\alpha} + \tilde{\xi}_\alpha) + z_\beta(\frac{R_r L_m}{L_r w_\sigma}\tilde{\psi}_{r\beta} - \frac{L_m}{w_\sigma}\tilde{Z}_\alpha + v_\beta + \\ &+ c_\beta z_\beta + c_\alpha \tilde{i}_{s\beta} + \tilde{\xi}_\beta) + \tilde{\psi}_{r\alpha}(-\tilde{Z}_\beta + v_{\psi\alpha}) + \tilde{\psi}_{r\beta}(\tilde{Z}_\alpha + v_{\psi\beta}) + \\ &+ \tilde{Z}_\alpha(-\hat{\omega}_r \tilde{Z}_\beta - \tilde{\omega}_r \hat{Z}_\beta + \tilde{\omega}_r \tilde{Z}_\beta + \tilde{\omega}_r \frac{R_r L_m}{L_r} i_{s\alpha} + \frac{R_r}{L_r}\tilde{Z}_\alpha + v_{Z\alpha}) + \\ &+ \tilde{Z}_\beta(\hat{\omega}_r \tilde{Z}_\alpha + \tilde{\omega}_r \hat{Z}_\alpha - \tilde{\omega}_r \tilde{Z}_\alpha + \tilde{\omega}_r \frac{R_r L_m}{L_r} i_{s\beta} + \frac{R_r}{L_r}\tilde{Z}_\beta + v_{Z\beta}).\end{aligned} \quad (46)$$

To ensure asymptotic stability, the Lyapunov condition (5) must be satisfied. This condition implies the $v_{\alpha,\beta}$ stabilizing current vector subsystem:

$$v_\alpha = -\frac{R_r L_m}{L_r w_\sigma}\tilde{\psi}_{r\alpha} - c_\alpha \tilde{i}_{s\alpha} - c_\beta z_\alpha - \tilde{\xi}_\alpha, \quad (47)$$

$$v_\beta = -\frac{R_r L_m}{L_r w_\sigma}\tilde{\psi}_{r\beta} - c_\alpha \tilde{i}_{s\beta} - c_\beta z_\beta - \tilde{\xi}_\beta, \quad (48)$$

and the flux vector subsystem properly:

$$v_{\psi\alpha} = k_\psi \tilde{Z}_\beta, \quad (49)$$

$$v_{\psi\beta} = -k_\psi \tilde{Z}_\alpha, \quad (50)$$

where $k_\psi$ is additionally introduced to $v_{\psi\alpha,\beta}$ gain.

Taking into account (47)–(50) in (46), one obtains:

$$\begin{aligned}\dot{V} &= -\frac{R_r}{L_r}(\tilde{\psi}_{r\alpha}^2 + \tilde{\psi}_{r\beta}^2) + \tilde{Z}_\alpha(-\hat{\omega}_r \tilde{Z}_\beta - \tilde{\omega}_r \hat{Z}_\beta + \tilde{\omega}_r \tilde{Z}_\beta + \\ &+ \tilde{\omega}_r \frac{R_r L_m}{L_r} i_{s\alpha} + \frac{R_r}{L_r}\tilde{Z}_\alpha - \frac{L_m}{w_\sigma} z_\beta + v_{Z\alpha}) + \tilde{Z}_\beta(\hat{\omega}_r \tilde{Z}_\alpha + \\ &+ \tilde{\omega}_r \hat{Z}_\alpha - \tilde{\omega}_r \tilde{Z}_\alpha + \tilde{\omega}_r \frac{R_r L_m}{L_r} i_{s\beta} + \frac{R_r}{L_r}\tilde{Z}_\beta + \frac{L_m}{w_\sigma} z_\alpha + v_{Z\beta})\end{aligned}. \quad (51)$$

To satisfy condition (5) the Z-subsystem correction terms should be defined:

$$v_{Z\alpha} = k_Z\left(-\frac{R_r}{L_r}\tilde{Z}_\alpha + \frac{L_m}{w_\sigma} z_\beta\right), \quad (52)$$

$$v_{Z\beta} = k_Z\left(-\frac{R_r}{L_r}\tilde{Z}_\beta - \frac{L_m}{w_\sigma} z_\alpha\right). \quad (53)$$

Taking into account the terms (49)–(50) in (52)–(53) the new form is obtained:

$$v_{Z\alpha} = k_Z\left(\frac{R_r}{L_r} v_{\psi\beta} + \frac{L_m}{w_\sigma} z_\beta\right), \quad (54)$$

$$v_{Z\beta} = k_Z\left(\frac{R_r}{L_r} v_{\psi\alpha} - \frac{L_m}{w_\sigma} z_\alpha\right), \quad (55)$$

where $k_Z$ is additionally introduced to $v_{\psi\alpha,\beta}$ gain.

The observer correction terms are strongly coupled to each other. The flux and Z-subsystem are coupled by (49)–(50) and the current subsystem is coupled by the error deviations (39)–(40). Such an observer structure guarantees better control system properties, especially near the very low speed. This case will be studied in more depth in the next section.

### B. The adaptive method of rotor speed estimation

The rotor angular speed can be treated as a parameter; therefore (51) should be rebuilt to the following form:

$$\dot{V} = \tilde{\omega}_r\left(\tilde{Z}_\alpha(\hat{Z}_\beta - \tilde{Z}_\beta) - \frac{R_r L_m}{L_r}(\tilde{Z}_\alpha i_{s\alpha} + \tilde{Z}_\beta i_{s\beta}) - \tilde{Z}_\beta(\hat{Z}_\alpha - \tilde{Z}_\alpha)\right) + \frac{1}{\gamma}\tilde{\omega}_r \dot{\tilde{\omega}}_r. \quad (56)$$

To satisfy the Lyapunov condition, the estimated rotor angular speed should be determined from:

$$\dot{\hat{\omega}}_r = \gamma_1\left(\tilde{Z}_\alpha(\hat{Z}_\beta - \frac{R_r L_m}{L_r}\hat{i}_{s\alpha}) - \tilde{Z}_\beta(\hat{Z}_\alpha + \frac{R_r L_m}{L_r}\hat{i}_{s\beta})\right), \quad (57)$$

where $\gamma_1$ is the constant gain $\gamma_1 > 0$ and there is the assumption that in (17) $d\omega_r / d\tau = 0$.

The method presented in this section is based on the adaptive approach. The gain $\gamma_1$ should be properly chosen so that the estimation speed observer deviation will be zero. The speed observer convergence depends on the $\gamma_1$ and $c_{\alpha,\beta}$ gains. In (49)–(50) and (52)–(55) the constant tuning gains $k_{\psi,\ Z} > 0$ and $k_\psi<1$ are introduced. The influence on the observer backstepping stability will be shown in Section V.

The $\tilde{Z}_{\alpha,\beta}$ deviations can be obtained from (31)–(32). On the other hand, the $\tilde{Z}_{\alpha,\beta}$ deviations can be obtained as follows without additional differential equations:

$$\tilde{Z}_\alpha = \hat{Z}_\alpha - \hat{\omega}_r \hat{\psi}_{r\alpha}, \quad (58)$$

$$\tilde{Z}_\beta = \hat{Z}_\beta - \hat{\omega}_r \hat{\psi}_{r\beta}. \quad (59)$$

### C. The non-adaptive method of rotor speed estimation

The previous section contains the adaptive approach to the angular speed reconstruction. In this section, the non-adaptive approach will be shown. Taking into account (19)–(20), multiplying properly by the rotor flux vector components and then summing both sides, the estimated rotor speed can be achieved in the same manner as in [2, 3]:

$$\hat{\omega}_{rr} = \frac{\hat{Z}_\alpha \hat{\psi}_{r\alpha} + \hat{Z}_\beta \hat{\psi}_{r\beta}}{\hat{\psi}_{r\alpha}^2 + \hat{\psi}_{r\beta}^2}. \quad (60)$$

In order to distinguish the adaptive and non-adaptive approaches, the estimated speed is indexed $\hat{\omega}_{rr}$ but in the speed observer (21)–(26) $\hat{\omega}_r = \hat{\omega}_{rr}$ (when the non-adaptive approach is used).

### D. The improved adaptive method of rotor speed estimation

In the adaptive estimation approach [18, 27, 36], the speed observer may have a problem with the low speed rotor reverse. The control system can be unstable. Therefore, the differentiated Lyapunov function will be rebuilt to the following form:

$$\dot{V} = -\gamma_1 \tilde{\omega}_{rr}^2 + \tilde{\omega}_r\left(\begin{aligned}\tilde{Z}_\alpha(\hat{Z}_\beta - \tilde{Z}_\beta) - \frac{R_r L_m}{L_r}(\tilde{Z}_\alpha i_{s\alpha} + \tilde{Z}_\beta i_{s\beta}) - \tilde{Z}_\beta(\hat{Z}_\alpha - \tilde{Z}_\alpha) + \\ + \frac{1}{\gamma}\dot{\tilde{\omega}}_r + \gamma_1 \tilde{\omega}_{rr}\end{aligned}\right), \quad (61)$$

where

$$\tilde{\omega}_{rr} = \hat{\omega}_r - \hat{\omega}_{rr}. \quad (62)$$

In (62) $\hat{\omega}_{rr}$ is given in (60).

The estimated rotor angular speed can be obtained by the improved differential equation:

$$\dot{\hat{\omega}}_r = \gamma_1\left(\tilde{Z}_\alpha(\hat{Z}_\beta - \frac{R_r L_m}{L_r}\hat{i}_{s\alpha}) - \tilde{Z}_\beta(\hat{Z}_\alpha + \frac{R_r L_m}{L_r}\hat{i}_{s\beta}) - \gamma_2 \tilde{\omega}_{rr}\right), \quad (63)$$

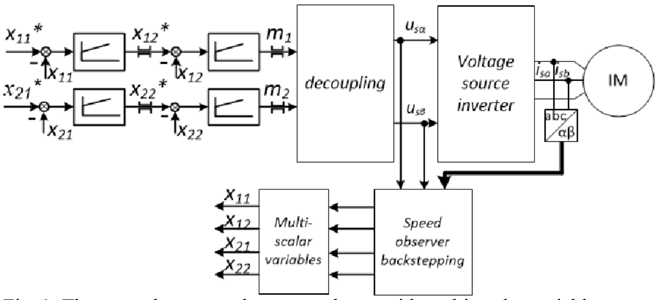

Fig. 1. The sensorless control system scheme with multi-scalar variables

where $\gamma_2 = \gamma_1$.

Finally, the Z-type speed observer backstepping structure is built using eight differential equations: (21)–(26), (41)–(42) with the correction terms (49)–(50), (54)–(55) and the estimated speed observer formula (57), (60) or (63).

The sensorless control system structure is presented in fig. 1. All the variables and structure blocks are presented in the Appendix section.

## V. Stability Analysis of the Speed Observer

The presented backstepping approach is based on the Lyapunov function CLF (control of Lyapunov function) [19]. The correction terms (49)–(50), (54)–(55) are chosen in such a manner to satisfy the Lyapunov condition (5). This condition guarantees the asymptotic stability of the observer system if the constant gains are $c_{\alpha,\beta}$, $\gamma_{1,2} > 0$. If these gains are $c_{\alpha,\beta}$, $\gamma_{1,2} >> 0$, then the observer is stiff [19] but the estimated rotor speed has more oscillations. The oscillations can lead to the observer working unstably. The gains move the system trajectory (the real poles) near to zero on the real axis (Re) or keep it away from the zero point (each real pole must be < 0 for the system to be stable). These observer gains influence the speed observer convergences. In the non-linear system literature, the backstepping observer convergence is proved by the Lassale-Yoshizawa theorem or Barbalat's Lemma [19]. These convergence theories are based on sets theory. If the set of solutions of the backstepping observer is bounded and the Lyapunov condition (5) is satisfied, then each solution is converged to the positive bounded solution set.

The other situation is with the $k_{\psi,Z}$ gains. The $k_{\psi,Z}$ should be $k_{\psi,Z}>0$ but only $k_\psi<1.0$ p.u. The $k_\psi$ must be smaller than 1.0 because for each $k_\psi \geq 1.0$ the flux subsystem is unstable.

In order to examine the impact of the observer gains, the non-linear system is linearized near the equilibrium point. The linearized system has the general form [40]:

$$\frac{d}{dt}\Delta x(t) = \mathbf{A}\Delta x(t) + \mathbf{B}\Delta u(t),\ \Delta x(t_0) = x(t_0) - x_n(t_0) \tag{64}$$

where **A**, **B** are the Jacobian matrices.

In the estimator presented in Section IV.A, B can be linearized near the equilibrium point and the matrix **A** is defined as:

$$\mathbf{A} = \begin{bmatrix} -(c_\beta + c_\alpha) & -\omega_\psi & 0 & 0 & 0 & a_3 & a_4 & 0 & 0 \\ \omega_\psi & -(c_\beta + c_\alpha) & 0 & 0 & -a_3 & 0 & 0 & a_4 & 0 \\ 0 & 0 & -a_1 & 0 & 0 & a_{12} & 0 & 0 & 0 \\ 0 & 0 & 0 & -a_1 & -a_{12} & 0 & 0 & 0 & 0 \\ 0 & k_Z a_3 & 0 & 0 & a_5 & -\omega_r & 0 & k_Z c_\beta a_3 & a_8 \\ -k_Z a_3 & 0 & 0 & 0 & \omega_r & a_5 & -k_Z c_\beta a_3 & 0 & a_9 \\ 1 & 0 & 0 & 0 & 0 & 0 & -c_\beta & \omega_\psi & 0 \\ 0 & 1 & 0 & 0 & 0 & 0 & -\omega_\psi & -c_\beta & 0 \\ 0 & 0 & 0 & 0 & a_{10} & a_{11} & 0 & 0 & 0 \end{bmatrix}$$

$$a_1 = \frac{R_r}{L_r},\ a_2 = \frac{R_r L_m}{L_r},\ a_3 = \frac{L_m}{w_\sigma},\ a_4 = c_\alpha c_\beta + \omega_\psi^2 - 1,$$

$$a_5 = \frac{R_r}{L_r}(1 - k_Z),\ a_8 = \omega_\psi a_2 i_{sd} - \hat{Z}_q,\ a_9 = \hat{Z}_d + \omega_\psi a_2 i_{sq},$$

$$a_{10} = \gamma_1(\hat{Z}_q - a_2 i_{sd}),\ a_{11} = -\gamma_1(\hat{Z}_d + a_2 i_{sq}),\ a_{12} = (k_\psi - 1).$$

The estimator system is oriented with the rotor flux vector $\vec{\psi}_r$, so $\psi_{rd} = |\vec{\psi}_r|$ and $\psi_{rq} = 0$ and the stator current vector components and $\omega_\psi$ can be treated as follows:

$$i_{sd} = \frac{\psi_{rd}}{L_m},\ i_{sq} = \frac{T_L}{a_5 \psi_{rd}},\ \omega_\psi = a_2\left(\frac{i_{sq}}{\psi_{rd}} + \omega_r\right).$$

The stability analysis for the adaptive speed observer is presented in Figs. 2 to 7. In Fig. 2 the eigenvalues of the linearized observer system while the rotor speed is changing from -1.0 to 1.0 p.u are shown.

For adaptive cases (Figs 2 to 4) for $\omega_r$=0 the eigenvalues are zero or near to zero. For this working point, the speed observer has the state variable oscillations (but is still stable).

The adaptive speed observer is unstable for the gains $c_\beta$<0.1 (Fig. 4).

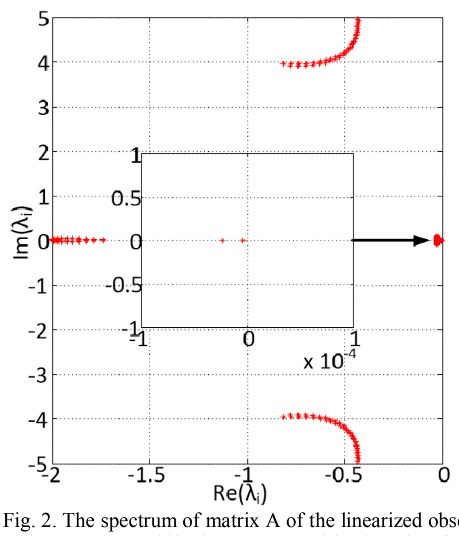

Fig. 2. The spectrum of matrix A of the linearized observer system for $c_\alpha$=1.0, and $c_\beta$=0.1 p.u. while the rotor speed is changing from -1.0 to 1.0 p.u. and $\gamma_1$=0.1 p.u., $k_\psi$=0.9, $k_Z$=1.0 p.u., adaptive rotor speed estimation (57)

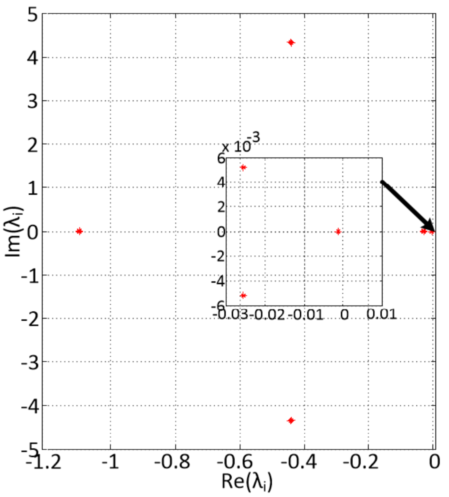


Fig. 3. The spectrum of matrix A of the linearized observer system for $c_\alpha$=1.0, and $c_\beta$=0.1 p.u. while the load torque is changing from 0 to 0.7 p.u., $\omega_r$=0.02 and $\gamma_1$=10, $k_\psi$=0.9, $k_Z$=1.0 p.u., adaptive rotor speed estimation (57)

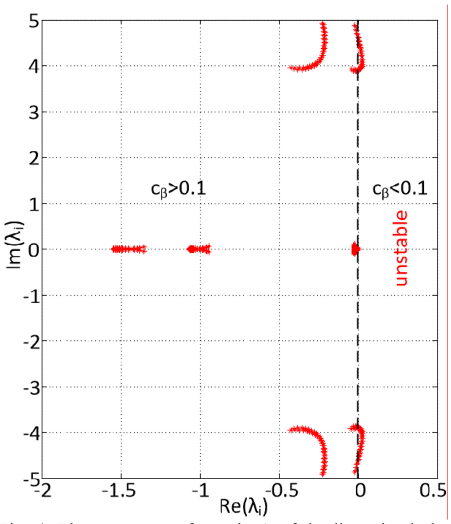


Fig. 4. The spectrum of matrix A of the linearized observer system for $k_\psi$=0.9, $k_Z$=1.0, $c_\alpha$=1.0 p.u. while the $c_\beta$ is changing from 0.01 to1.0 and the rotor speed from -1.0 to 1.0 p.u., adaptive rotor speed estimation (57)

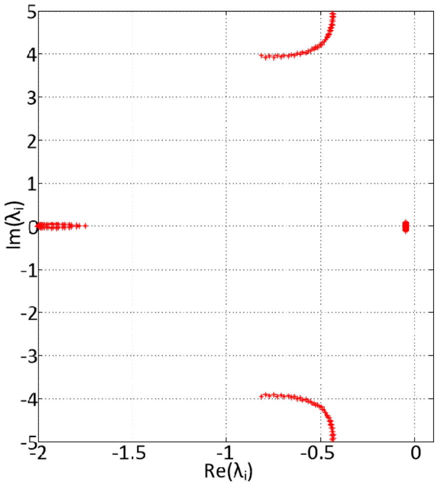


Fig. 5. The spectrum of matrix A of the linearized observer system for $c_\alpha$=1.0, and $c_\beta$=1 p.u. while the rotor speed is changing from -1.0 to 1.0 p.u. and, $k_\psi$=0.9, $k_Z$=1.0 p.u., non-adaptive or improved adaptive estimation

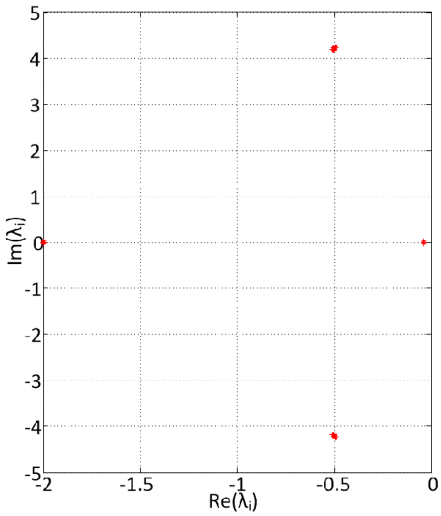


Fig. 6. The spectrum of matrix A of the linearized observer system for $c_\alpha$=1.0, and $c_\beta$=0.1 p.u. while the load torque is changing from 0 to 0.7 p.u., $\omega_r$=0.02 and $\gamma_1$=1, $k_\psi$=0.9, $k_Z$=1.0 p.u., non-adaptive or improved adaptive estimation

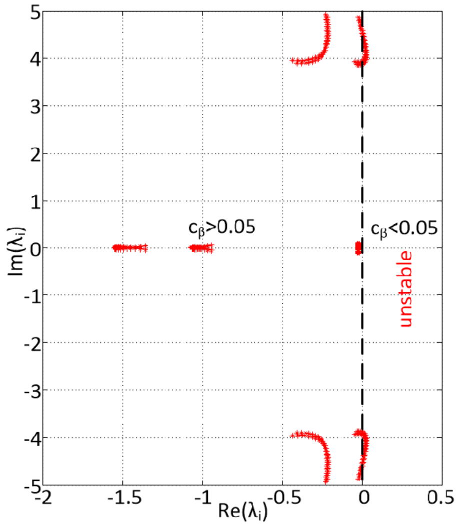


Fig. 7. The spectrum of matrix A of the linearized observer system for $k_\psi$=0.9, $k_Z$=1.0, $c_\alpha$=1.0, $\gamma_1$=1 p.u. while the $c_\beta$ is changing from 0.01 to 2.0 and the rotor speed from -1.0 to 1.0 p.u., non-adaptive or improved adaptive estimation

The second analysis case is the non-adaptive estimation method or improved adaptive speed estimation. For this case, the estimated speed is from (60) or (63). In (63) the adaptive and non-adaptive approach is applied. It has been named "improved" because the speed observer has better properties than only the adaptive. The analysis for this case is shown in Figs. 5 to 7. Figs. 2–4 and 5–7 can be compared with each other. The non-adaptive estimation or improved adaptive estimation methods are better than the purely adaptive method. For each analysis case in Figs 5–7, the eigenvalues of the linearized observer system are near to zero but are not actually zero. For these cases, the eigenvalues are more negative than for the adaptive method. The $k_\psi$ gain value change is not presented in Figs. 1–7. This value is constant $k_\psi$=0.9 and should always be $k_\psi$<1.0. The $k_\psi$ must be smaller than 1.0 because if it is not, the observer flux subsystem is unstable. If $k_\psi$=1.0 then the flux subsystem differential equation structure is changed. In (23) the positive coupling occurs from the element $+\hat{\omega}_r\hat{\psi}_{r\beta}$ (for $\hat{\omega}_r\hat{\psi}_{r\beta} > 0$). In (24) the negative coupling occurs from $-\hat{\omega}_r\hat{\psi}_{r\beta}$ (for $\hat{\omega}_r\hat{\psi}_{r\beta} > 0$). Accordingly, the flux subsystem has a different form than the mathematical model and for $k_\psi \geq 1.0$ the speed observer backstepping is unstable.

The $k_z$ gain value was $k_z$=1.0 p.u. for both cases.

In the next sections the experimental results for the non-adaptive speed estimation method will be shown (due to their better speed observer properties than adaptive estimation).

## VI. EXPERIMENTAL RESULTS

All tests were carried out in a 5.5 kW drive system. The motor drive system parameters are given in Table II. The control system was implemented in an interface with a *DSP Sharc* ADSP21363 floating point signal processor and Altera Cyclon 2 FPGA. The signal processor had 3 Mb SRAM, 333 MHz, 666 MIPS, 2GFLOPS. The transistor switching frequency was 10 kHz.

The *Runge Kutta IV* integration method was implemented with the speed observer. The control system calculations were about 15 µs without code machine optimization.

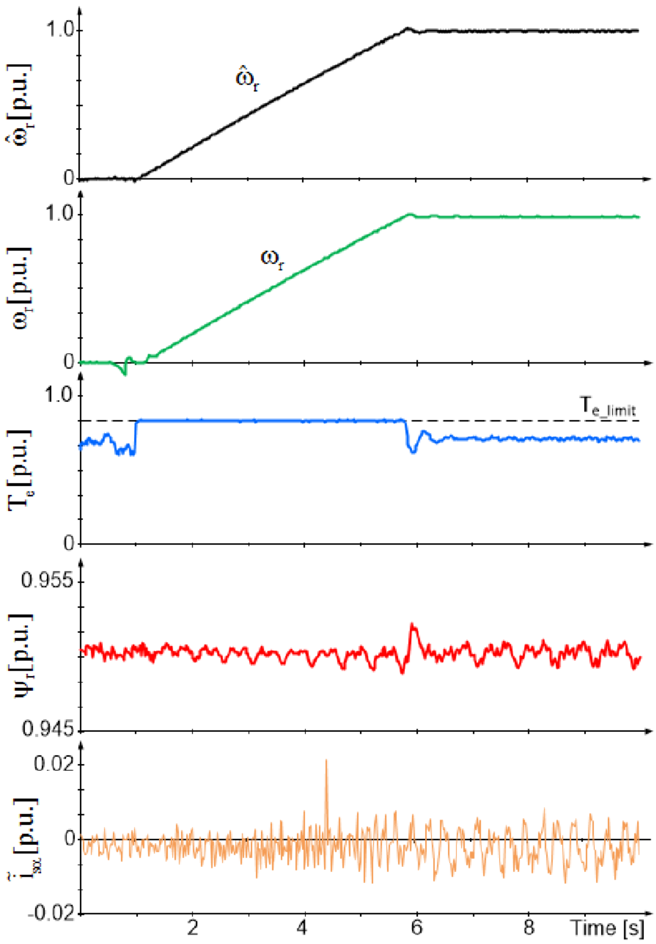


Fig. 8. Machine is starting up to 1.0, and the nominal load torque is applied ($T_e$~0.7 p.u.)

Based on stability analysis, and because of the poor properties of the Z-observer with the adaptive speed estimation approach from (57), the "clean" adaptive approach in the experimental investigations will not be taken into account.

The experimental section is divided into three subsections (Drive starting and speed reversal, Load rejection behaviour and Robustness against parameter detuning). Figs 8–16 present: estimated rotor speed $\hat{\omega}_r$, measured speed $\omega_r$, rotor flux module $\psi_r = \sqrt{\psi_{r\alpha}^2 + \psi_{r\beta}^2}$, estimated electromagnetic torque $\hat{T}_e$ and referenced load torque $T_{e\_set}$, stator current vector components errors.

### A. Drive starting and speed reversal

The drive starting from standstill with rated torque is shown in fig.8, while the speed reversal from 1.pu to - 1.pu is described in fig. 9. In fig. 10 the machine is starting up to 2.5 p.u. The speed was limited to 2.5 p.u. because of the mechanical resonance problem in the drive system. In fig. 11, very slow speed reversing from 0.01 to -0.01 is shown. The multi-scalar variables $x_{12}$, $x_{21}$ and the rotor speed error are presented.

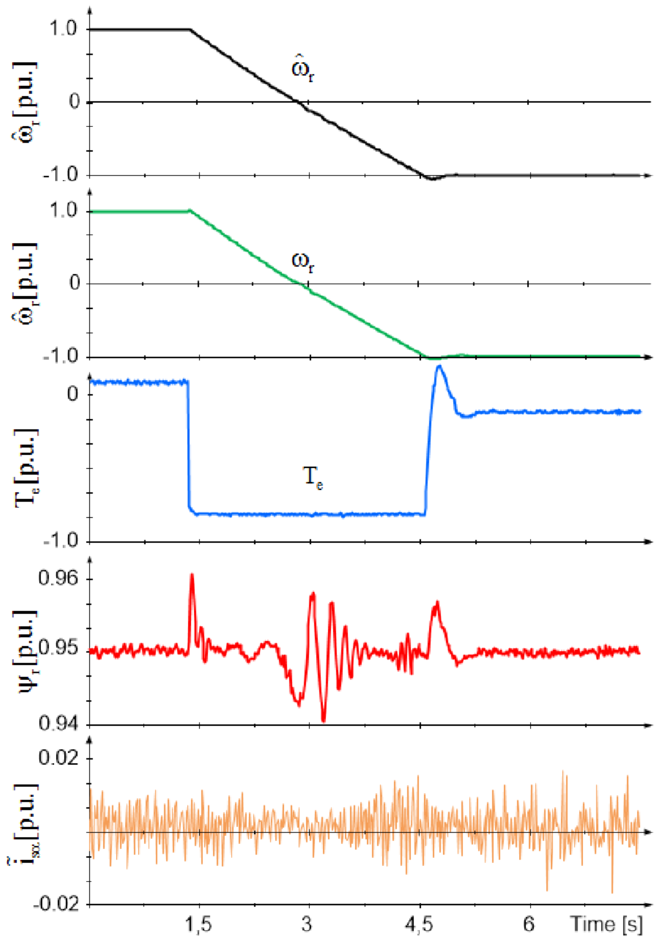


Fig. 9. Machine is reversing from 1.0 to -1.0, without load torque command

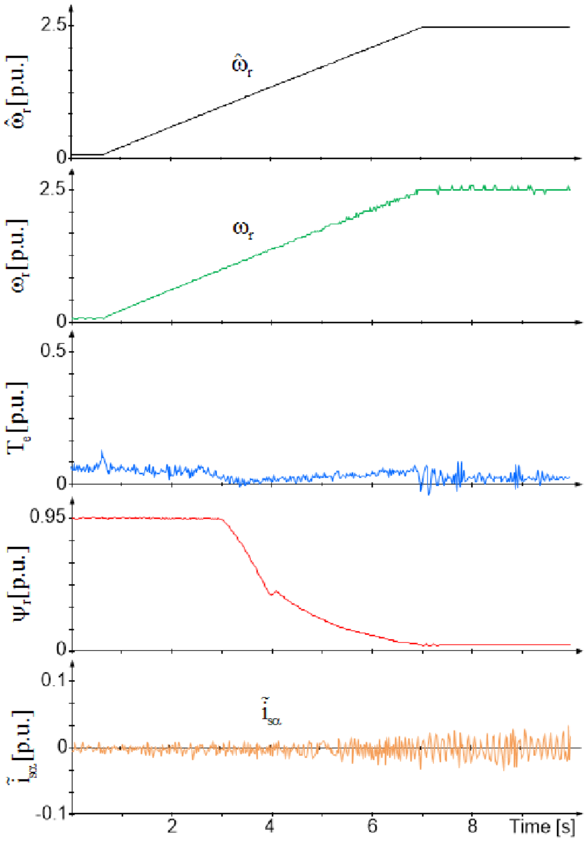


Fig. 10. Machine is starting up to 2.5, without load torque command

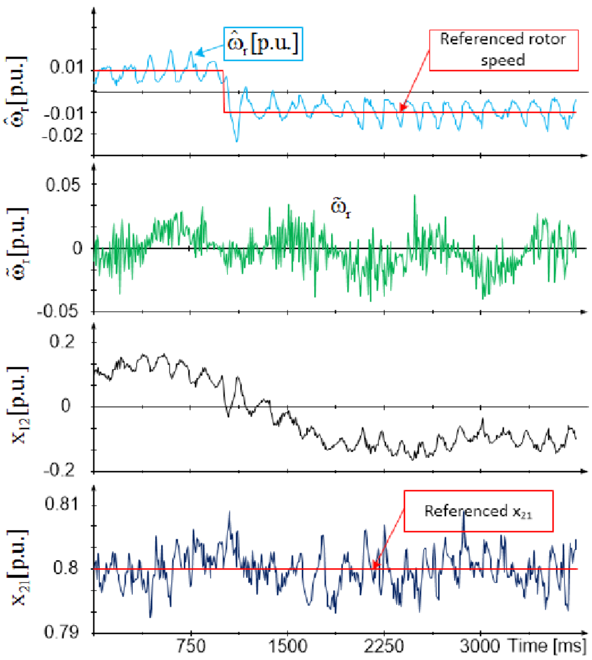


Fig. 11. Experimental transients: estimated rotor speed, rotor speed error, $x_{12}$, $x_{21}$

## B. *Load rejection behaviour*

In this section, the control system behaviour on the load torque command is tested. In fig. 12, load torque is on and off and the referenced speed is zero. The control system worked stably.

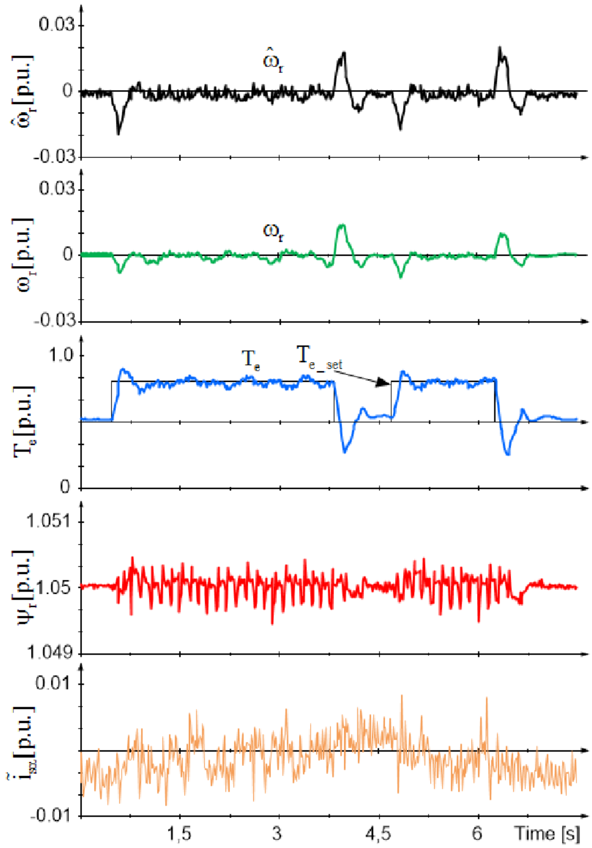


Fig. 12. The sensorless control load rejection behaviour. The reference speed is zero. The nominal load torque is turned on and off

## C. *Robustness against parameter detuning*

In this section the robustness against IM parameter detuning is presented. In fig. 13, the stator resistance $R_s$ is changed about 30% and the rotor resistance $R_r$ is changed to about 50% of nominal value. The reference speed is zero. The nominal load torque is applied. This test shows that for zero speed and nominal torque command, if the IM parameters are detuned then the control system is stable but the properties are not sufficient. The electromagnetic torque occurs the limit ($T_e$*_limit*) and the rotor speed is not properly stabilized. The speed observer is not robust if the IM parameters ($R_s$, $R_r$) change above 30% (at nominal load torque and zero speed operation). The stable work of the sensorless control system is guaranteed if the resistance changes are below 25% or if the 25% nominal load torque is applied or the reference speed is different to the zero speed. This case is shown in fig. 14. The reference speed is 0.02 p.u. and the load torque and the resistance changes are the same as for the case presented in fig. 13. For the reference speed 0.02 p.u. the sensorless control system works stably for the resistance detuning and load nominal torque changes.

In fig. 15 the IM main inductance $L_m$ is changed about 10% of the nominal value. The reference speed is zero. With changes of $L_m$ below 15% the sensorless control system works stably.

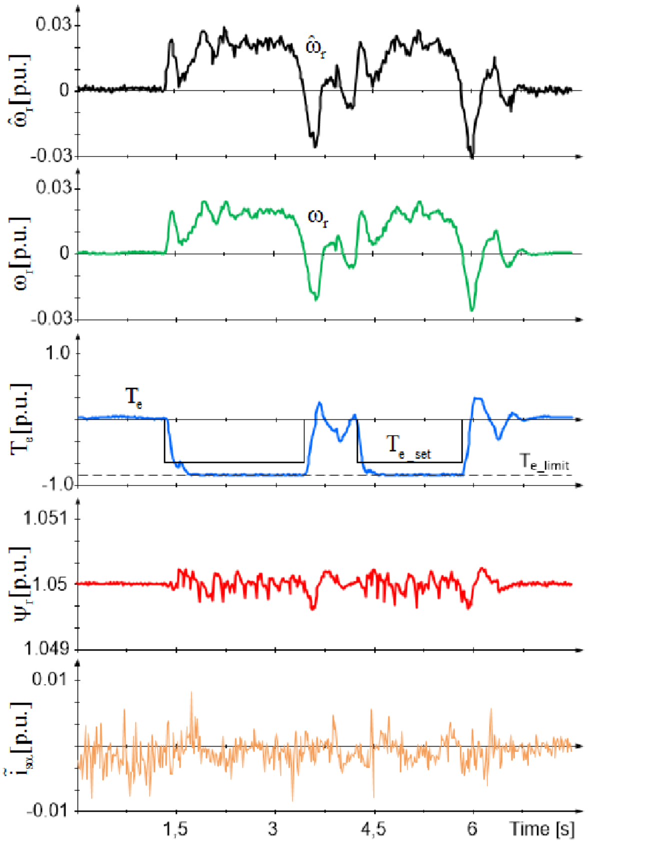


Fig. 13. The IM parameters are changed: $R_s$ to about 30% and $R_r$ to about 50% of nominal values. The reference speed is zero

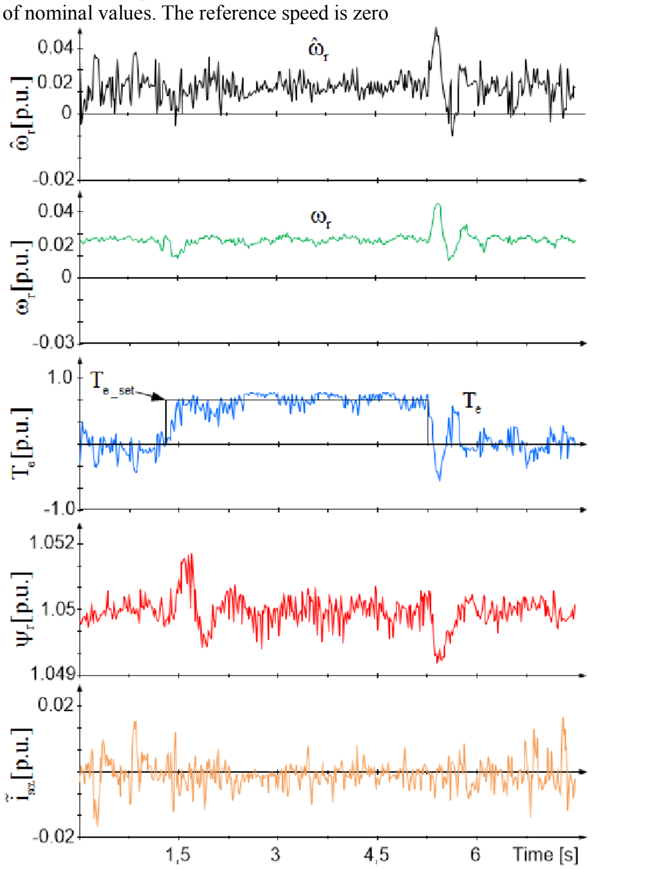


Fig. 14. The IM parameters are changed: $R_s$ to about 30% and $R_r$ to about 50% of nominal values. The reference speed is 0.02 p.u.

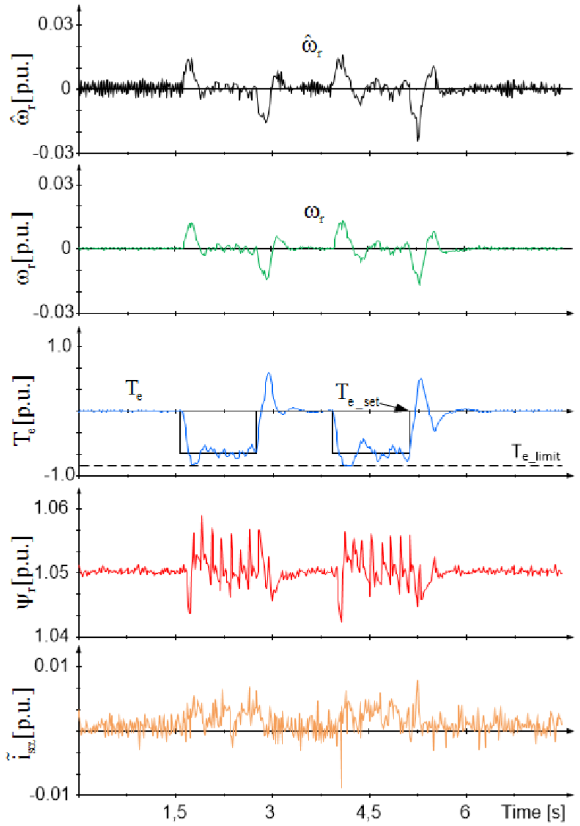


Fig. 15. The IM main inductance $L_m$ is detuned about 10%

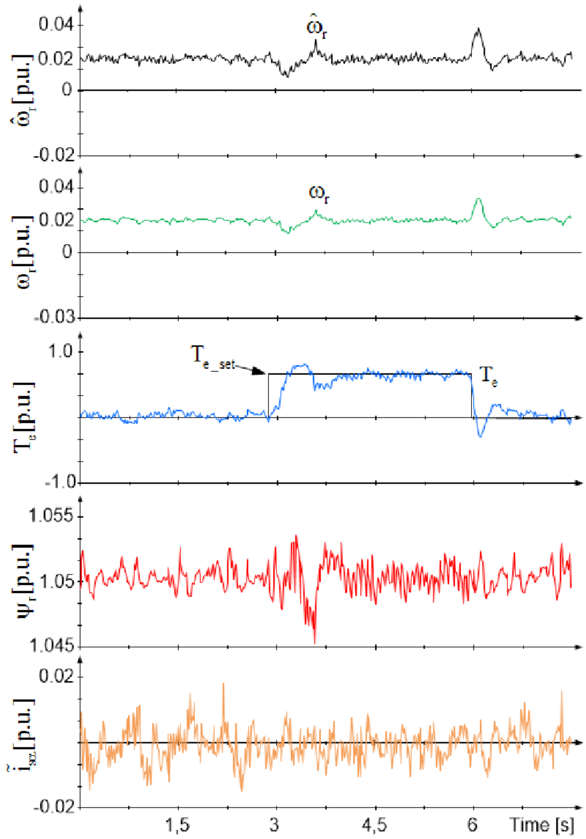


Fig. 16. The IM main inductance $L_m$ is detuned about 20%

In fig. 16 the reference speed is 0.02 p.u. and the IM main inductance $L_m$ is detuned about 20%. The sensorless control system works stably.

In experimental tests, the gains were chosen according to the method presented in Section V: $c_\alpha$=1, $c_\beta$=1, $\gamma_1$=$\gamma_2$=0.5, $k_\psi$=0.85, $k_Z$=1.0 p.u.

The motor parameters are presented in Table II. More machine tests and the standard deviations of the estimated rotor speed and the stator current vector components are presented in Table I.

Table I. The machine reverse tests

| Test | $\sigma(\tilde{\omega}_r)$ | $\sigma(\tilde{i}_{s\alpha})$ | $\sigma(\tilde{i}_{s\beta})$ |
|---|---|---|---|
| 1 | 0.015621 | 0.015120 | 0.015512 |
| 2 | 0.01101 | 0.012488 | 0.013201 |
| 3 | 0.01020 | 0.01201 | 0.012063 |
| 4 | 0.01010 | 0.00451 | 0.00512 |
| 5 | 0.01311 | 0.00626 | 0.00718 |
| 6 | 0.05103 | 0.02810 | 0.03156 |
| 7 | 0.04109 | 0.02749 | 0.02910 |

σ – standard deviation;
The machine tests:
Test 1 – $\hat{\omega}_r = 0.01 ... -0.01$ p.u.
Test 2 – $\hat{\omega}_r = 0.02 ... -0.02$ p.u;
Test 3 – $\hat{\omega}_r = 0.1 ... -0.1$ p.u;
Test 4 – $\hat{\omega}_r = 0.5 ... -0.5$ p.u;
Test 5 – $\hat{\omega}_r = 1 ... -1$ p.u.;
Test 6 – $\hat{\omega}_r = 0.1$ p.u., and $R_s$ and $R_r$ were chosen as 50% respect to their rated values,
Test 7 – $\hat{\omega}_r = 1.0$ p.u., and $R_s$ and $R_r$ were chosen as 50% respect to their rated values.

In Tests 6 and 7, robust tests on the stator and rotor resistance changes were carried out. The stator and rotor resistances were changed to 50% of the nominal machine resistances. The rotor angular speed was estimated by the non-adaptive approach, the speed estimation error was 0.05 p.u. (5%) in the stationary state, and the reference speed was 0.1 p.u. (Test 6) and 1.0 p.u (Test 7).

## VII. Conclusions

This paper describes the novel structure of the rotor angular speed observer, named *Z,* for an induction machine. This structure was obtained by use of backstepping synthesis and an adaptive mechanism. The proposed estimators are characterized by ease of selection of the gains and the small rotor angular speed error estimation < 0.03 p.u. in the dynamic states. This error value depends on a kind of machine working point.

The author proposed the backstep through the integrator structure. The standard integrator backstepping structure, developed to the control system, was shown by the authors of the backstepping approach in [19]. In this paper, the integrator structure is used to obtain the Z-type adaptive observer backstepping. The Z-type observer structure has additional stabilizing elements in the differential equations which make it less oscillatory. In the Z-type observer, the rotor speed can be estimated in three ways: the adaptive, the non-adaptive, and the improved adaptive approaches. The "clean" adaptive with

TABLE II
The squire-cage parameters and references unit

| Symbol | Quantity | Values |
|---|---|---|
| $R_s$ | stator resistance | 2.92 Ω/0.045 p.u. |
| $R_r$ | rotor resistance | 3.36 Ω/0.052 p.u. |
| $L_m$ | magnetizing inductance | 0.422 H/2.08 p.u. |
| $L_s$, $L_r$ | stator and rotor inductance | 0.439 H/2.17 p.u. |
| $L_\sigma$ | leakage inductance | 0.017 H/0.09 p.u. |
| $P_n$ | nominal power | 5.5 kW |
| $I_n$ | nominal stator current (Y) | 10.4 A |
| $U_n$ | nominal stator voltage (Y) | 400 V |
| n | nominal rotor speed | 2940 rpm |
| f | nominal frequency | 50 Hz |
| $U_b$=$U_n$ | reference voltage | 400 V |
| $I_b = I_n/\sqrt{3}$ | reference current | 6.01 A |
| $P_b$ | reference power | 1.6 kW |
| $T_{eb}$ | reference torque | 7.65 Nm |

the Z-type observer structure cannot be used in drive applications because the error estimated speed is higher than 5% near the zero speed.

The main advantages of the proposed Z-type observer structure are:

- The rotor speed is more accurately determined than in standard observer backstepping, especially at a low rotor speed;
- The Z-type observer state variables have smaller oscillations than in standard observer [2-3] and observer backstepping [21-22];
- The stability is guaranteed by the Lyapunov criteria;
- The Z-type and standard observers are relatively easy to tune using methods from Section V;
- The sensorless control system with the Z-type observer backstepping works stably for the zero speed command and nominal load torque changes;
- The Z-type observer is robust against IM resistance changes below 25% nominal value and main inductance $L_m$ changes below 15% when the rotor speed is zero and the machine is nominally loaded. For rotor speeds higher than zero or load torques of about 50% nominal IM parameters can be more detuned than above values;
- The proposed Z-type observer structure is more complicated than the standard observer backstepping but stability of the control system is provided over the whole speed range.

The proposed methodology, based on the extended observer structure and adaptive backstepping, gives new possibilities for the development of observer theory in electric drive systems.

The Z-type observer can be successfully used in industrial applications.

## Appendix

The control system with the multi-scalar variables is shown in Fig. 17. The multi-scalar variables were proposed in [40] and defined [39]:

$$x_{11} = \hat{\omega}_r \,, \tag{65}$$

$$x_{12} = \hat{\psi}_{r\alpha}\hat{i}_{s\beta} - \hat{\psi}_{r\beta}\hat{i}_{s\alpha} \,, \tag{66}$$

$$x_{21} = \hat{\psi}_{r\alpha}^2 + \hat{\psi}_{r\beta}^2 \,, \tag{67}$$

$$x_{22} = \hat{\psi}_{r\alpha}\hat{i}_{s\alpha} + \hat{\psi}_{r\beta}\hat{i}_{s\beta} \,. \tag{68}$$

The feedback linearizing controls (decoupling) are obtained, as follows:

$$u_1 = \frac{w_\sigma}{L_r}\left(\frac{1}{T_i}m_1 + x_{11}(x_{22} + \frac{L_m}{w_\sigma}x_{21})\right), \tag{69}$$

$$u_2 = \frac{w_\sigma}{L_r}\left(\frac{1}{T_i}m_2 - x_{11}x_{22} - \frac{R_r L_m}{w_\sigma L_r}x_{21} - \frac{R_r L_m}{L_r}i_s^2\right), \tag{70}$$

where $m_{1,2}$ are new introduced control variables and $T_i$ is defined as:

$$\frac{1}{T_i} = \frac{R_r L_s + R_s L_r}{w_\sigma}.$$

The IM control variables are determined:

$$u_{s\alpha} = \frac{\psi_{r\alpha}u_2 - \psi_{r\beta}u_1}{x_{21}}, \tag{71}$$

$$u_{s\beta} = \frac{\psi_{r\alpha}u_1 + \psi_{r\beta}u_2}{x_{21}}. \tag{72}$$

The Z-type speed observer structure is as follows:

$$\frac{d\hat{i}_{s\alpha}}{d\tau} = -a_{11}\hat{i}_{s\alpha} + a_{12}\hat{\psi}_{r\alpha} + a_{13}\hat{Z}_\beta + a_{14}u_{s\alpha} - \tilde{i}_{s\alpha}(c_\alpha + c_\beta) - \tilde{\xi}_\alpha(c_\alpha c_\beta + 1), \tag{73}$$

$$\frac{d\hat{i}_{s\beta}}{d\tau} = -a_{11}\hat{i}_{s\beta} + a_{12}\hat{\psi}_{r\beta} - a_{13}\hat{Z}_\alpha + a_{14}u_{s\beta} - \tilde{i}_{s\beta}(c_\alpha + c_\beta) - \tilde{\xi}_\beta(c_\alpha c_\beta + 1), \tag{74}$$

$$\frac{d\hat{\psi}_{r\alpha}}{d\tau} = -a_{21}\hat{\psi}_{r\alpha} + a_{22}\hat{i}_{s\alpha} + \hat{Z}_\beta(k_\psi - 1) - k_\psi\hat{\omega}_r\hat{\psi}_{r\beta}, \tag{75}$$

$$\frac{d\hat{\psi}_{r\beta}}{d\tau} = -a_{21}\hat{\psi}_{r\beta} + a_{22}\hat{i}_{s\beta} - \hat{Z}_\alpha(k_\psi - 1) + k_\psi\hat{\omega}_r\hat{\psi}_{r\alpha}, \tag{76}$$

$$\frac{d\hat{Z}_\alpha}{d\tau} = \frac{d\hat{\omega}_r}{d\tau}\hat{\psi}_{r\alpha} - \hat{\omega}_r(\hat{Z}_\beta - a_{22}\hat{i}_{s\alpha} - \hat{\psi}_{r\alpha}) + a_{13}(\tilde{i}_{s\beta} + c_\alpha\tilde{\xi}_\beta), \tag{77}$$

$$\frac{d\hat{Z}_\beta}{d\tau} = \frac{d\hat{\omega}_r}{d\tau}\hat{\psi}_{r\beta} + \hat{\omega}_r(\hat{Z}_\alpha + a_{22}\hat{i}_{s\beta} + \hat{\psi}_{r\beta}) - a_{13}(\tilde{i}_{s\alpha} + c_\alpha\tilde{\xi}_\alpha), \tag{78}$$

$$\frac{d\tilde{\xi}_\alpha}{d\tau} = \tilde{i}_{s\alpha}, \tag{79}$$

$$\frac{d\tilde{\xi}_\beta}{d\tau} = \tilde{i}_{s\beta}, \tag{80}$$

where

$$a_{11} = \frac{R_s L_r^2 + R_r L_m^2}{L_r w_\sigma}, a_{12} = \frac{R_r L_m}{L_r w_\sigma}, a_{13} = \frac{L_m}{w_\sigma}, a_{14} = \frac{L_r}{w_\sigma}, a_{21} = \frac{R_r}{L_r},$$

$$a_{22} = \frac{R_r L_m}{L_r}.$$

The rotor speed derivative in (77)–(78) can be determined from (63):

$$\frac{d\hat{\omega}_r}{d\tau} = \gamma_1\left(\tilde{Z}_\alpha(\hat{Z}_\beta - a_{22}\hat{i}_{s\alpha}) - \tilde{Z}_\beta(\hat{Z}_\alpha + a_{22}\hat{i}_{s\beta})\right). \tag{81}$$

The speed can be estimated with an adaptive approach from (63) or a non-adaptive approach from (60):

$$\hat{\omega}_r = \frac{\hat{Z}_\alpha\hat{\psi}_{r\alpha} + \hat{Z}_\beta\hat{\psi}_{r\beta}}{\hat{\psi}_{r\alpha}^2 + \hat{\psi}_{r\beta}^2}. \tag{82}$$


## ACKNOWLEDGMENT

The author would like to thank Prof. Krzeminski for the extended form of the exponential observer. Many thanks to Prof . Kokotovi´c, Prof. Krsti´c and Prof. Kanellakopoulos for the backstepping method which motivated the writing of this paper.


## REFERENCES


[1] B. Hafez, A.S. Abdel-Khalik, A.M. Massoud, S. Ahmed, R.D. Lorenz: Single-Sensor-Based Three-Phase Permanent-Magnet Synchronous Motor Drive System With Luenberger Observers for Motor Line Current Reconstruction, *IEEE Trans. Ind. Appl.*, Vol. 50, Issue 4, pp. 2602-2613, 2014.

[2] Z. Krzeminski: Observer of induction motor speed based on exact disturbance model, Power Electronics and Motion Control Conference, 13th EPE-PEMC, pp. 2294-2299, 2008.

[3] Z. Krzeminski, A. Lewicki, M. Morawiec: Speed observer based on extended model of induction machine, IEEE International Symposium on Industrial Electronics (ISIE), pp. 3107-3112, 2010.

[4] S. Roshany-Yamchi, M. Cychowski, R. R. Negenborn, B. De Schutter, K. Delaney, J. Connell: Kalman Filter-Based Distributed Predictive Control of Large-Scale Multi-Rate Systems: Application to Power Networks, *IEEE Trans. Control Sys. Tech.*, Vol. 20, Issue: 1, pp. 27-39, 2013.

[5] S. Jafarzadeh, C. Lascu, M.S. Fadali: State Estimation of Induction Motor Drives Using the Unscented Kalman Filter, *IEEE Trans. Ind. Electr.*, Vol. 59, Issue: 11, pp. 4207-4216, 2012.

[6] Si-Hun Jo, SeoEun Son, Soon Lee, Jung-Wook Park: Kalman-Filter-Based Multilevel Analysis to Estimate Electric Load Composition, *IEEE Trans. Ind. Electr.*, Vol. 59, Issue: 11, pp. 4263-4271, 2012.

[7] S. Tong, Yongming Li: Adaptive Fuzzy Output Feedback Tracking Backstepping Control of Strict-Feedback Nonlinear Systems With Unknown Dead Zones, *IEEE Trans. Fuzzy Sys.*, Vol. 20, Issue: 1, pp. 168-180, 2012.

[8] S. Tong, Yongming Li, Gang Feng, Tie-Shan Li: Observer-Based Adaptive Fuzzy Backstepping Dynamic Surface Control for a Class of MIMO Nonlinear Systems, Cybernetics, *IEEE Trans. Sys., Man., and Cyber.*, Vol.41, Issue: 4, pp. 1124-1135, 2011.

[9] S. Tong, Yongming Li, Peng Shi: Observer-Based Adaptive Fuzzy Backstepping Output Feedback Control of Uncertain MIMO Pure-Feedback Nonlinear Systems, *IEEE Trans. Fuzzy Sys.*, Vol. 20, Issue: 4, pp. 771-785, 2012.

[10] S. Tong, Y. Li, G. Feng, T. Li: Observer-based adaptive fuzzy backstepping dynamic surface control for a class of non-linear systems with unknown time delays, *IET Control Theory & Applications*, Vol. 5, Issue: 12, pp. 1426-1438, 2011.

[11] Yongming Li, Tieshan Li, Shaocheng Tong: Adaptive fuzzy backstepping dynamic surface control of uncertain nonlinear systems based on filters, International Conference on Information Science and Technology (ICIST), pp. 83-88, 2012.

[12] Tang Zhiguo, Xu Jing, Liu Keping, Li Yuanchun: An adaptive backstepping observer-controller design for manipulators cooperating flexible payload, 9th International Conference on Fuzzy Systems and Knowledge Discovery (FSKD), pp. 2343-2347, 2012.

[13] Q. Zhou, P. Shi., S. Xu, H. Li: Observer-Based Adaptive Neural Network Control for Nonlinear Stochastic Systems With Time Delay, *IEEE Trans. Neur. Net. and Learn. Sys.*, Vol: 24 , Issue: 1, pp. 71-80, 2013.

[14] Chih-Hong Lin, Ming-Kuan Lin, Ren-Cheng Wu: Integral Backstepping Control for a PMSM Drive Using Adaptive RNN Uncertainty Observer, International Symposium on Computer, Consumer and Control (IS3C), pp. 777-780, 2012.

[15] Chih-Hong Lin, Ming-Kuan Lin, Ren-Cheng Wu, Shi-Yan Huang: Integral backstepping control for a PMSM drive using adaptive FNN uncertainty observer, IEEE International Symposium on Industrial Electronics (ISIE), pp. 668-673, 2012.

[16] Chih-Hong Lin, Ren-Cheng Wu, Chong-Chi Chong: Adaptive backstepping control for a PMSM drive using RFNN uncertainty observer, 6th IEEE Conference on Industrial Electronics and Applications (ICIEA), pp. 62-67, 2011.

[17] Y. Wen, X. Ren: Observer-based fuzzy adaptive control for non-linear time-varying delay systems with unknown control direction, *IET Control Theory & Applications*, Vol. 4, Issue: 12, pp. 2757-2769, 2010.

[18] C. Schauder: Adaptive speed identification for vector control of induction motors without rotational transducers, *IEEE Trans. Ind. Appl.*, Vol.: 28, Issue: 5, pp. 1054 -1061, 1992.

[19] M. Krsti´c, I. Kanellakopoulos, and P. Kokotovi´c, *Nonlinear and Adaptive Control Design*, Wiley-Interscience Publication 1995.
[20] F. A. Payam, B. M. Dehkordi: Nonlinear Sliding-Mode Controller for Sensorless Speed control of DC servo Motor Using Adaptive Backstepping Observer, PEDES, pp. 1-5, 2006.
[21] M. Jalalifar, A.F. Payam, B. Mirzaeian, S.M.S. Nezhad: Dynamic Modeling and Simulation of an Induction Motor with Adaptive Backstepping Design of an Input-Output Feedback Linearization Controller in Series Hybrid Electric Vehicle, International Conference on Power Electronics, Drives and Energy Systems, pp. 1-6, 2006.
[22] M. Morawiec: The Adaptive Backstepping Control of Permanent Magnet Synchronous Motor Supplied by Current Source Inverter, *IEEE Trans. Ind. Inf.*, Vol. 9, Issue: 2, pp. 1047-1055, 2013.
[23] R. Trabelsi, A. Kheder, M.F. Mimouni, F. M'sahli: Backstepping control for an induction motor with an adaptive Backstepping rotor flux observer, 18th Mediterranean Conference on Control & Automation (MED), pp. 5-10, 2010.
[24] Chao Zhang, Zongji Chen, Chen Wei: Nonlinear flight control design using sliding mode disturbance observer-based constraint backstepping, 10th World Congress on Intelligent Control and Automation, pp. 1818-1825, 2012.
[25] H. Aschemann, R. Prabel, D. Schindele: Observer-based backstepping control of an electro-pneumatic clutch, American Control Conference (ACC), pp. 509 -514, 2012.
[26] Bin-Feng Yu, Han Yan, Hai-Bo Ji: Integrated guidance and control based on backstepping and high-gain observers, 31st Chinese Control Conference (CCC), pp. 4739-4744, 2012.
[27] Qiao Jihong, Li Zihao, Wang Hongyan: Adaptive sliding mode control with nonlinear disturbance observer for uncertain nonlinear system based on backstepping method, 10th World Congress on Intelligent Control and Automation (WCICA), pp. 1609-1614, 2012.
[28] Lu Kunfeng, Xia Yuanqing, Fu Mengyin, Deng Zhihong: Observer-based control for stochastic jump systems via backstepping method, 30th Chinese Control Conference (CCC), pp. 5947-5952, 2011.
[29] N. Djeghali, M. Ghanes, S. Djennoune, J. Barbot: Backstepping fault tolerant control based on second order sliding mode observer: Application to induction motors, 50th IEEE Conference on Decision and Control and European Control Conference, pp. 4598-4603, 2011.
[30] X. Yang Simon, Anmin Zhu, Guangfeng Yuan, M.Q.-H. Meng: A Bioinspired Neurodynamics-Based Approach to Tracking Control of Mobile Robots, *IEEE Trans. Ind. Electr.*, Vol.: 59 , Issue: 8, pp. 3211-3220, 2012.
[31] Yinsong Wang, Xinghuo Yu: New Coordinated Control Design for Thermal-Power-Generation Units, *IEEE Trans. Ind. Electr.*, Vol.: 57 , Issue: 11, pp. 3848-3856, 2010.
[32] M. Hajian, J. Soltani, G.A. Markadeh, S. Hosseinnia: Adaptive Nonlinear Direct Torque Control of Sensorless IM Drives With Efficiency Optimization, *IEEE Trans. Ind. Electr.*, Vol.: 57 , Issue: 3, , pp. 975-985, 2010.
[33] Yi Jin, Pyung Hun Chang, Maolin Jin, Dae Gab Gweon: Stability Guaranteed Time-Delay Control of Manipulators Using Nonlinear Damping and Terminal Sliding Mode, *IEEE Trans. Ind. Electr.*, Vol.: 60, Issue: 8, pp. 3304-3317, 2013.
[34] Yao Sun, Mei Su, Xing Li, Hui Wang, Weihua Gui: Indirect Four-Leg Matrix Converter Based on Robust Adaptive Back-Stepping Control, *IEEE Trans. Ind. Electr.*, Vol.: 58 , Issue: 9, pp. 4288-4298, 2011.
[35] Yeong-Hwa Chang, Wei-Shou Chan, Chia-Wen Chang: T-S Fuzzy Model-Based Adaptive Dynamic Surface Control for Ball and Beam System, *IEEE Trans. Ind. Electr.*, Vol.: 60 , Issue: 6, pp. 2251-2263, 2013.
[36] H. Kubota, I. Sato, Y. Tamura, K. Matsuse, H. Ohta, Y. Hori, Regenerating-mode low-speed operation of sensorless induction motor drive with adaptive observer, *IEEE Trans. Ind. Applic*., vol. 38, no. 4, pp. 1081-1086, pp. 1081-1086, 2002.
[37] M. Ghanes, A. Glumineau, J. De Leon: Backstepping observer validation for sensorless induction motor on low frequencies benchmark, Industrial Technology, IEEE ICIT '04. 2004 IEEE International Conference on, Vol. 3, pp. 1368 - 1373, 2004.
[38] Ramzi Trabelsi, Adel Kheder, Med Faouzi Mimouni,Faouzi M'sahli: Sensorless Speed and Flux Control Scheme for an Induction Motor with an Adaptive Backstepping Observer, 7th International Multi-Conference on Systems, Signals and Devices, pp. 1-7, 2010.
[39] Z. Krzeminski: Nonlinear control of induction motor. Proceedings of the 10th IFAC World Congress, pp. pp. 349-354, Munich 1987.
[40] S. Antman, P. Holmes, K.R. Sreenivasan: *Texts in Applied Mathematics* Volume 2, ISSN: 0939-2475, pp 5-19, 2003.

**Marcin Morawiec** received the M.Sc. degree in electrical engineering from Czestochowa University of Technology, Czestochowa, Poland in 2003 and Ph.D. degree from Gdansk University of Technology, Gdansk, Poland in 2007. Since 2008, he has been an Assistant Professor with Gdansk University of Technology. He is author of over 50 articles and 2 books, 1 Polish patent and 5 patent applications. His main scientific activities are concentrated on multi-scalar models of any electrical machines, sensorless control, nonlinear control, backstepping control and an adaptive observer backstepping.